Improved Spacecraft Tracking and Navigation Using a Portable Radio Science Receiver

Melissa Soriano, Christopher Jacobs,
Robert Navarro, Charles Naudet,
Stephen Rogstad, Leslie White,
Susan Finley, Charles Goodhart,
Elliott Sigman, Joseph Trinh
Jet Propulsion Laboratory
California Institute of Technology
Pasadena, CA 91109
818-393-7632
Melissa.A.Soriano@jpl.nasa.gov

Juan Lobo Garcia, Cristina García-Miró
INTA/NASA
Madrid Deep Space Communications Complex
Madrid, Spain

Mattia Mercolino, Roberto Maddè
European Space Agency
European Space Operations Center
Darmstadt, Germany

Abstract— **The Portable Radio Science Receiver (PRSR) is a suitcase-sized open-loop digital receiver designed to be small and easy to transport so that it can be deployed quickly and easily anywhere in the world. The PRSR digitizes, down-converts, and filters using custom hardware, firmware, and software. Up to 16 channels can be independently configured and recorded with a total data rate of up to 256 Mbps. The design and implementation of the system's hardware, firmware, and software is described. To minimize costs and time to deployment, our design leveraged elements of the hardware, firmware, and software designs from the existing full-sized operational (non-portable) Radio Science Receivers (RSR) and Wideband VLBI Science Receivers (WVSR), which have successfully supported flagship NASA deep space missions at all Deep Space Network (DSN) sites.**

We discuss a demonstration of the PRSR using VLBI, with one part per billion angular resolution: 1 nano-radian / 200 µas synthesized beam. This is the highest resolution astronomical instrument ever operated solely from the Southern Hemisphere. Preliminary results from two sites are presented, including the European Space Agency (ESA) sites at Cebreros, Spain and Malargüe, Argentina. Malargüe's South American location is of special interest because it greatly improves the geometric coverage for spacecraft navigation in the Southern Hemisphere and will for the first time provide coverage to the 1/4 of the range of declination that has been excluded from reference frame work at Ka-band.

TABLE OF CONTENTS

1. INTRODUCTION 1
2. HARDWARE DESIGN AND IMPLEMENTATION ..3
3. FIRMWARE DESIGN AND IMPLEMENTATION ...4
4. SOFTWARE DESIGN AND IMPLEMENTATION....5
5. PRSR OPERATIONS.....6
6. ANALYSIS OF CEBREROS DATA.....6
7. ANALYSIS OF MALARGÜE DATA 7
8. CONCLUSION.....8
9. ACKNOWLEDGEMENTS.....8
REFERENCES.....9

1. INTRODUCTION

Interplanetary navigation uses four primary types of measurements for orbit determination: Range, Doppler, Delta Differential One-way Range, and onboard optical. Range is a measurement of the distance to the spacecraft and is obtained using the difference in time between when a signal is sent and received. Doppler is a measurement of the radial velocity of the spacecraft using the Doppler shift of the signal [1]. Delta Differential One-Way (DOR) range is a measurement of the angular position and velocity of the spacecraft using station-differenced one-way range [2]. These angular measurements are referenced to a predetermined catalog of radio sources. These radio reference sources are quasars that are located in distant galaxies and have very stable positions [3]. Onboard optical measurements use the spacecraft camera to image a target against a star background and are useful for approaching a target such as a comet that does not have well known ephemeris with respect to quasars.

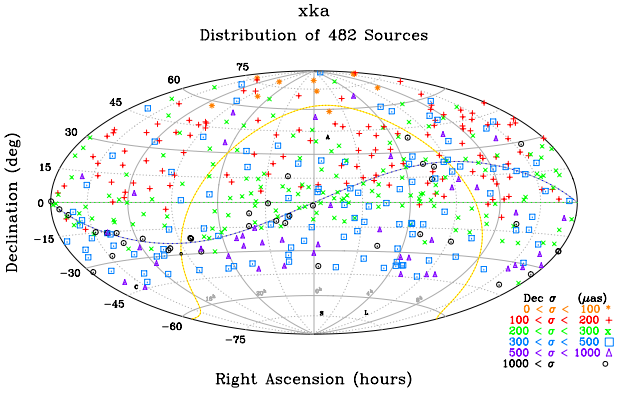

Figure 1- Current distribution of X/Ka radio sources

The current distribution of X/Ka band radio sources is shown in Figure 1 [4]. This plot uses the Hammer-Aitoff projection, which preserves the surface area density of

978-1-4673-1813-6/13/$31.00 ©2013 IEEE

sources. The yellow dotted line is the galactic plane and the blue dashed line is the ecliptic plane. Points are colored based on 1-sigma standard deviation declination errors. The current requirement for Delta-DOR accuracy is < 200 µas and includes orange (< 100 µas) and red (100-200 µas) points. Accurate Delta-DOR measurements are particularly important for missions landing on another planet.

The NASA Interior Exploration using Seismic Investigations, Geodesy and Heat Transport (InSight) mission will place a lander on Mars to study the planet's interior. Launch is scheduled in early 2016 and landing in late 2016. Insight is planning to approach Mars at 18 hours right ascension and -26 degrees declination. There are few sources in this region of the sky that meet current Delta-DOR accuracy requirements.

Navigation measurements such as Delta-DOR are performed using the Deep Space Network (DSN), the ground portion of the communications link between Earth and NASA spacecraft. As shown in **Figure 2**, the DSN has three Deep Space Communications Complexes (DSCCs), located at Goldstone, California, Madrid, Spain, and Canberra, Australia. The DSCCs are positioned in such a way that the DSN can have at least one station in view of a spacecraft at any given time. The DSCCs currently form two baselines, shown as solid lines. The potential Canberra-Madrid baseline is too long to provide sufficient mutual visibility and thus is not used. The visibility on the Goldstone-Madrid baseline shrinks to zero for sources below -25° declination. An additional station in Argentina would add three more baselines, shown in **Figure 2** as dotted/dashed lines. These new baselines would improve the radio catalog in the southern hemisphere and allow Delta-DOR measurements with an accuracy of < 200 µas for use by the InSight mission.

Figure 2- X/Ka stations for celestial reference frame

Each DSCC has one 70-m dish antenna, multiple 34-m antennas, and related hardware. This hardware includes various types of full rack-sized open-loop and closed-loop receivers. Closed-loop receivers are efficient for characterizing slowly changing signals and are the tools used for operational ranging and Doppler orbit-determination processes. However, closed-loop receivers require a tone or carrier to lock onto. Delta-DOR measurements rely on observations of both the spacecraft and a distant reference source that cannot be tracked by a closed-loop receiver. Open-loop receivers are needed for these types of applications. Open-loop receivers can utilize downlink frequency predicts as input from navigation to compensate for expected Doppler shift. DSN open-loop receivers include the Radio Science Receiver (RSR), Very-Long Baseline Interferometry (VLBI) Science Receiver (VSR), Wideband VLBI Science Receiver (WVSR), and the Portable Radio Science Receiver (PRSR). Key properties are shown in **Table 1** [5].

Table 1- Key properties of DSN open-loop receivers

Open-Loop Receiver	Inputs	Input bandwidth	Max number of channels	Max recording rate	Size
RSR	2	110 MHz	4	64 Mbps	DSN rack
VSR	2	110 MHz	16	84 Mbps	DSN rack
WVSR	2	500 MHz	16	256 Mbps	DSN rack
PRSR	1	500 MHz	16	256 Mbps	2.5 U

The RSR is an open-loop receiver used for radio science. Radio science experiments utilize precise measurements of small changes in phase, frequency, and amplitude in the spacecraft signal to infer properties of planets and satellites and measure gravitational fields [5]. The RSR has also supported many critical spacecraft events with high signal dynamics such as Mars Science Laboratory (MSL) Entry, Descent, and Landing (EDL) [6]. Each DSCC has at least two RSRs.

The WVSR is an open-loop receiver dedicated to Delta Differential One-way Range (Delta-DOR) measurements. It has supported spacecraft tracking for many of NASA's flagship missions, such as Mars Science Laboratory. As shown in **Table 1**, the WVSR supports a wider input bandwidth of 500 MHz, an increased number of channels, and higher recording rates than the RSR. Each DSCC has two WVSRs.

The Portable Radio Science Receiver design leveraged elements of the hardware, firmware, and software designs of the RSR and WVSR [7]. The PRSR has a few key differences from the RSR and WVSR. First, it has a much smaller form factor that allows it to be transported easily (4" x 17" x 20" in height, width, depth), as shown in **Figure 3**. Second, to minimize size and complexity, the PRSR accepts only a single IF input. However, two PRSRs can be used to support dual band experiments. Third, the PRSR uses a

978-1-4673-1813-6/13/$31.00 ©2013 IEEE

laptop computer rather than a rack-mounted server to run its high-level monitoring and control software.

Figure 3- Portable Radio Science Receivers at JPL lab

In this paper, we present an overview of the PRSR system and discuss its use at the Cebreros, Spain and Malargüe, Argentina ESA stations to reduce the Delta-DOR error budget and therefore provide improved spacecraft navigation. Hardware, firmware, and software design and implementation are discussed in Sections 2, 3, and 4 respectively. In Section 5, we describe PRSR operations and installation, as well as several applications. In Sections 6 and 7 respectively, results from PRSR experiments with the Cebreros, Spain and Malargüe, Argentina ESA stations are discussed. Finally, in Section 8, conclusions are reached.

2. HARDWARE DESIGN AND IMPLEMENTATION

The PRSR hardware is implemented using three sub-assemblies: an Intermediate Frequency Digitizer (IFD) that is responsible for digitizing the input analog IF, a Real-time Signal Processer (RSP) that performs down conversion, filtering, and channelization, and a Data Processor and Controller (DPC) that configures, monitors, and controls the other subsystems and stores the recorded data. A system block diagram is shown in **Figure 4**.

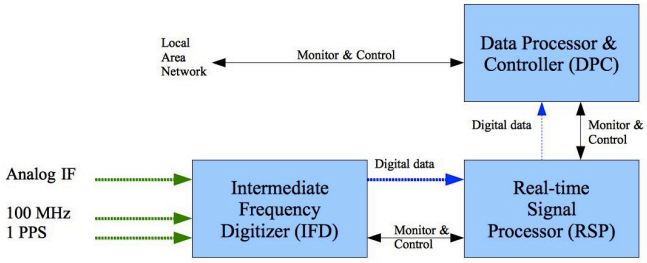

Figure 4- PRSR system block diagram

Intermediate Frequency Digitizer

An analog signal at Intermediate Frequency (IF) of 100-600 MHz is the primary input to the system. The Intermediate Frequency Digitizer (IFD) samples this analog signal at 1280Ms/s. The sampling rate of 1280 MHz was chosen as the lowest possible sampling rate that would allow the design of an anti-aliasing filter with 1 db cutoff at 600 MHz, image rejection of at least 30 dB, and group delay variation of less than 0.2 dB [10].

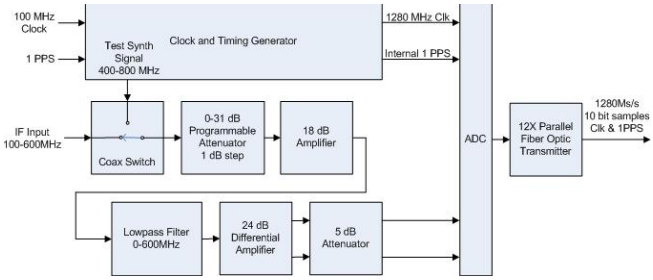

Figure 5- IFD block diagram

A block diagram of the IFD is shown in **Figure 5**. The IFD accepts a 100 MHz reference clock and 1 Pulse Per Second (1 PPS) timing reference. The Clock and Timing Generator (CTG) generates a 1280 MHz sampling clock from the 100 MHz clock. It also generates an internal 1 PPS from the 100 MHz clock which is synchronized to the 1 PPS reference. In addition, the CTG generates a test signal.

At the front of the signal path, a coaxial switch allows selection of either the input signal or the test signal. A programmable attenuator (0 - 31 dB in 1 dB steps) allows adjustment of the signal level being applied to the analog-to-digital converter (ADC). The signal is then amplified, band pass filtered, and transformed into a differential signal before being input into the ADC. The IFD digital output is provided on a 12X parallel fiber optic cable. The IFD also includes a Rabbit 3000 microprocessor that is responsible for monitoring and control.

Real-time Signal Processor

The digital data from the IFD is provided to the Real-time Signal Processor (RSP), which downconverts, filters, and channelizes the digital data. Up to 16 channels may be configured, with bandwidths of 1 kHz – 40 MHz and 1-16 bits per sample. The maximum recommended aggregate recording rate for all configured channels of the system is 256 Mbps. The data from each channel is recorded to disk for real time monitoring and post processing analysis.

The RSP was implemented on a 15-layer custom printed circuit board, the Advanced TCA Processor Engine (APE) board. The APE Board includes 5 Virtex-II Xilinx Field Programmable Gate Arrays (FPGAs). The APE board also includes a PPC440Gx processor that is responsible for monitoring and control. The APE PPC communicates using TCP/IP with the DPC that provides the monitoring and

978-1-4673-1813-6/13/$31.00 ©2013 IEEE

control interface to the PRSR system. The APE PPC also communicates with the IFD Rabbit microprocessor using TCP/IP for monitoring and control.

3. Firmware Design and Implementation

System Description

The FPGA firmware design receives one digitized intermediate frequency input as 1280 MHz, 8-bit samples and provides as output up to sixteen independent, digitally tuned and downconverted channels over a wide range of output sampling bandwidths and bit precisions. The largest output bandwidth is 40 MHz complex samples and the smallest output bandwidth is 1 kHz complex output samples. To accommodate this wide range of output bandwidths, a two step approach for downconversion is used. A block diagram of this approach is shown in Figure 6. The first step involves a seven channel polyphase filterbank with two times oversampling. This produces seven frequency fixed wideband channels of 160 MHz complex bandwidth with 80 MHz spacing between the channels. The channels are centered at frequencies of 80, 160, 240, 320, 400, 480 and 560 MHz. A channel at 0 or 640 MHz is not produced.

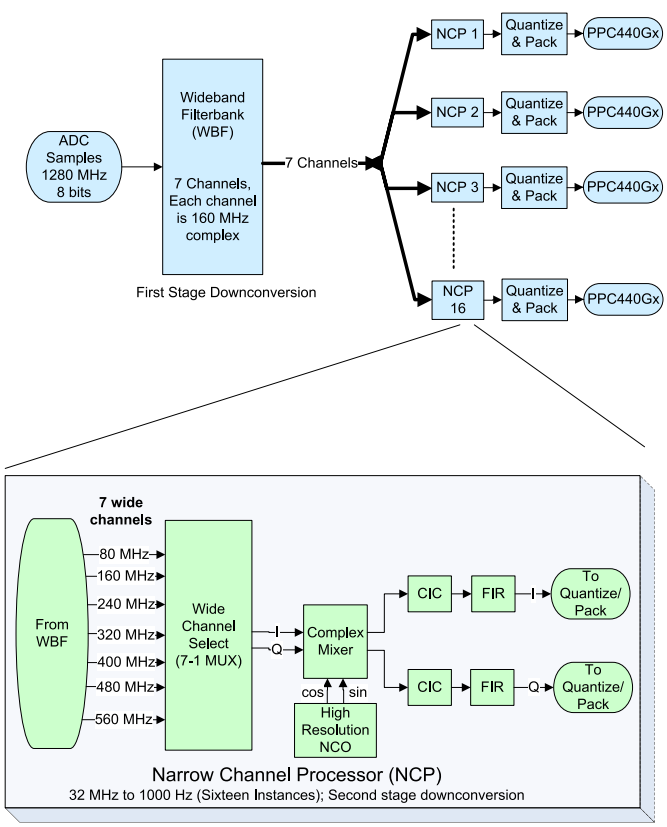

Figure 6- Firmware channel processing

The next step of the downconversion sends all seven wideband channels to sixteen independent narrow band channel tunable downconverters. Each of the sixteen narrow band channels uses a multiplexor circuit to choose the wideband 160 MHz channel of interest. The overlapping of the bands allows a spacecraft signal to be followed even if it drifts in frequency due to Doppler shift. The signal of interest is digitally mixed to baseband with a numerically controlled oscillator/modulator that receives phase and frequency updates once per millisecond. This allows the downconverter to follow a polynomial model of the predicted Doppler shifted frequency profile of a spacecraft signal.

After shifting the signal to baseband, a cascade of two downconverting digital filters decimates to the desired output recording bandwidth. The first digital filter is a Cascaded Integrate and Comb (CIC) filter. These multiplier free Finite Impulse Response (FIR) filters are highly efficient when making large reductions in sample rate. The second stage filter is a adjustable coefficient FIR filter with variable decimation factors from 1 to 16. In addition to providing additional decimation, it acts as a compensation filter for the sin(x)/x frequency domain response of the CIC filter. Finally, each channel has a module to quantize the output to the desired number of bits per sample and pack the samples into FPGA buffer memory for transfer to the PPC440Gx.

Wideband Filter bank

A downconverting wideband polyphase FIR filter has been developed to process input data in the 0 – 640 MHz range which has been sampled at a 1280 Msample/sec rate. The polyphase FIR divides this data into 7 overlapping bands which are 160 MHz wide with a 160 Msample/sec rate and downconverts these bands to a center frequency of 0 Hz. The response of this downconverting polyphase FIR is shown in **Figure 7**. The overlapping bands make it possible to extract narrower bands anywhere in the range of 25 to 615 MHz without any FIR amplitude rolloff. Each of the output bands of the Polyphase FIR is effectively a downconverting mixer followed by a 64-tap FIR.

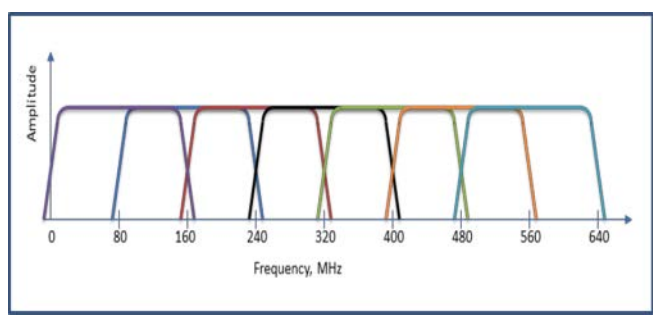

Figure 7 - Overlapping Wideband Channels

Narrowband Channel Processing

Each narrowband channel first uses a 7 to 1 multiplexor to choose the wideband channel containing the frequency band of interest. Next, a Numerically Controlled Oscillator (NCO) is used to mix the center of the band of interest to 0

978-1-4673-1813-6/13/$31.00 ©2013 IEEE

Hz. The NCO accepts phase and frequency updates once a millisecond from the PPC. The millisecond update rate together with the ability to control both phase and frequency from the PPC enables high precision control of the NCO and allows a high order polynomial phase model to be followed for purposes such as Doppler compensation of objects in deep space.

Narrow band channel processing is accomplished using two stages of filtering. The first stage is a high decimation (decimation factor of 2 to 10000) 3rd order CIC Filter. The second stage is a parallel tap symmetric FIR filter with variable decimation factors from 1 to 16. The number of taps for this second filter is always 16 times the decimation factor with a maximum of 256 taps available. This arrangement allows the decimation of the input sampling rate of 160 MHz to be anywhere from 80 MHz to 1 kHz (although 80 MHz is not supported operationally). Another important feature is the ability to change decimation rates without reprogramming the FPGA.

The CIC filter provides for very high decimation rates, but does not provide for sharp cutoffs or flat frequency responses in the passband. The FIR filter has limited decimation rates, but can provide passbands that are flat, with only 0.05 dB of ripple, over 85% of the sampling bandwidth. Also, attenuation in the stopband is at least 50 dB for decimation factors greater than two. For decimation by 1, the FIR only provides compensation for the CIC passband shape and the stopband attenuation is essentially that of the CIC filter.

Recorded Data

The outputs of each narrowband channel are complex samples of greater than 16 bits in both the in-phase and quadrature components. Each channel has a data packing and buffering module that interfaces with the PPC and facilitates flexible data recording. Complex sample components can be quantized to 16, 8, 4, 2 or 1 bit. The quantization is accomplished by truncation and numbers are meant to be later interpreted by multiplying by two and adding one. This 2n+1 transformation eliminates the DC offset introduced by truncation of two's-complement number systems. Next, these samples are packed into FPGA memory buffers. The buffers are sized to hold up to 1 millisecond worth of samples and the PPC retrieves these samples via DMA access each millisecond when triggered via interrupt. This data is written to the DPC disk.

4. SOFTWARE DESIGN AND IMPLEMENTATION

Data Processor and Controller

The DPC is responsible for monitoring and controlling the system, interfacing with other DSN/ESA systems, and storing the recorded data on disk. The DPC software is implemented on a laptop computer, running the Debian Linux operating system, that communicates with the RSP using TCP/IP protocol. The DPC also provides monitoring and control of the IFD through the RSP as shown in **Figure 4**. Navigation may provide downlink frequency predicts which contain predicted center frequencies for the target signal. The DPC software parses these predicts and calculates a set of phase and frequency values that allow a NCO to remove Doppler shifts and mix the signal of interest to baseband. These values are updated and sent to the RSP every second. Command channel links are used to communicate using an ASCII command/response protocol. Depending on the command, the DPC software process will communicate with the IFD and/or RSP. The DPC software is also responsible for providing real-time displays, including time vs. frequency Fast Fourier Transforms (FFT) and carrier Power-to-Noise (Pc/No) plots.

Intermediate Frequency Digitizer

The IFD's Rabbit microprocessor configures, monitors, and controls the IFD. This microprocessor operates at 29.4 MHz and includes 512K static Random Access Memory (RAM) and 512K flash memory. The software was written in ZWorld's Dynamic C, which is based on the C language and utilizes its own set of libraries. These libraries include user-callable functions that facilitate multitasking, network communication, and embedded assembly code.

The IFD monitor & control interface is via a network socket connection and uses an ASCII command/response protocol. The IFD responds on both the standard telnet port and a special reboot port. Up to two connections on the telnet port and a simultaneous connection on the reboot port to the same IFD unit are supported. New versions of the IFD monitor & control software can be loaded to the Rabbit processor via ftp, facilitating upgrades if needed.

Real-time Signal Processor

The Real-time Signal Processor's PPC440Gx interfaces to the FPGAs using a Linux kernel device driver that maps FPGA registers to user space memory and allows direct memory access for high performance when transferring downconverted samples from the FPGA to the PPC440Gx. In addition, the device driver responds to interrupts from the RSP hardware, keeping the software and firmware synchronized. The RSP software is real-time and is responsible for delivering phase and frequency models to the firmware every second. The RSP software is also responsible for reading data from the firmware in real-time and writing this data to files on the DPC using a Direct Memory Access (DMA) engine in the PPC.

The RSP monitoring and control interface is via a network socket connection and utilizes an ASCII command/response protocol. Multiple successive command/response interactions are allowed on a connection. Multiple simultaneous connections are allowed, with resource contention resolved within the device driver.

978-1-4673-1813-6/13/$31.00 ©2013 IEEE

5. PRSR OPERATIONS

Operations Concept

The PRSR is designed to be easy to use and flexible. Its uses to date include the Mars Science Laboratory (MSL) Entry, Descent, and Landing (EDL), Gravity Recovery And Interior Laboratory (GRAIL), and VLBI. One key element to the PRSRs success has been its portability. For MSL, a PRSR was deployed for testing with MSL test bed in preparation for EDL. Another PRSR was sent to Parkes, Australia and recorded MSL's UHF signal during EDL. For VLBI, a PRSR travelled overseas to the Cebreros, Spain and Malargüe, Argentina ESA stations, where measurements were made to demonstrate potential improvements to the radio source catalog.

Mars Science Laboratory Entry, Descent, and Landing

The full rack-sized Radio Science Receivers located at the DSN Canberra complex received real-time communications during MSL EDL. In preparation for this operational usage, testing took place at the Jet Propulsion Laboratory using the MSL test bed, which includes a Small Deep Space Transponder (SDST) engineering model. The SDST X-band signal was down-converted to IF, converted to digital data, transmitted across JPL from the MSL test bed to a lab via a fiber optic cable, converted back to analog IF, and then fed as input to a PRSR. A single 100 MHz channel was configured and centered based on expected received frequencies. During EDL operational readiness, the PRSR received and recorded EDL X-band communications. These records were streamed and processed in real-time by the EDL Data Analysis (EDA) system. The PRSR's portability made it possible to test the EDA with the MSL test bed.

Gravity Recovery And Interior Laboratory

The Gravity Recovery and Interior Laboratory (GRAIL) mission consisted of two spacecraft, in orbit around the moon and separated by 175-225 kilometers, which mapped the gravity field of the moon by measuring the changes in distance between the spacecraft using Ka-band radio signals. Four PRSR receivers were delivered to the GRAIL mission. One receiver is operational at each Deep Space Communications Complex and these three PRSRs continue to serve as backups for the RSRs. The GDSCC PRSR was placed in the pedestal of a 34-meter antenna and was used to receive signals that were sent between the two GRAIL spacecraft in order to detect any communication problems. The fourth PRSR was built as a spare.

VLBI

The VLBI technique creates a phased array with antennas clocked to independent frequency standards. When measuring angular positions of either spacecraft or quasars, the strength of the VLBI measurement scales with baseline length. We are seeking to leverage the portability of the PRSR in order to access antennas very distant from our current operational sites.

The ESA currently has two operational deep space antennas and a third one was recently completed. Deep Space Antenna 01 (DSA01) is located in New Norcia, Australia and Deep Space Antenna 02 (DSA02) is located in Cebreros, Spain. Deep Space Antenna 03 (DSA03) is located in Malargüe, Argentina and became operational on January 6, 2013. All three are 35-m beam wave-guide antennas [8]. In Sections 6 and 7, we present results from VLBI demonstrations with the previously operational DSA02 near Cebreros, Spain and the new DSA-03 in Malargüe, Argentina.

Future Development

A future version of the PRSR could use Commercial Off The Shelf (COTS) technology very similar, or identical, to that currently being used at JPL to develop antenna arraying systems. With this relatively low-cost technology, the next generation PRSR has the potential to shrink to a 1-U chassis while providing comparable performance and sensitivity at a fraction of the cost of the original. This next-generation PRSR could be deployed to support navigation for the InSight mission.

6. ANALYSIS OF CEBREROS DATA

Data

After several short tests to verify the PRSR to DSA02 interfaces, we collected data on DOY 201 of 2012, pairing the DSN 34-m waveguide antenna in Madrid, Spain, DSS-55, with the Cebreros station. The overlap between the DSN and ESA Intermediate Frequencies (IF) is 420 to 600 MHz. We recorded Ka-band (32 GHz) with 16 channels of 4-MHz wide data at 2-bit resolution spanning 180 MHz. Signal correlation was done with SOFTC [11] and fringe fitting was done with CFIT, which is a modernized version of Lowe's FIT code [12]. Radio observations at Ka-band vs X-band have several advantages: sources are significantly more compact, and therefore have more stable positions, and ionospheric and solar plasma effects are reduced [4]. The schedule included 5 strong quasars spread over all 4 quadrants of azimuth that we cycled through 3 times. These 15 targets had sufficient geometric diversity to allow us to estimate the Cebreros to DSS 55 baseline to about 2cm (1-sigma) per 3-D baseline component. This precision meets our current requirements.

In order to measure system stability, we tracked a single strong quasar for 2000 sec. We were able to detect the quasar with integrations as short as 1 second. The resulting 2000 time samples were used to determine an Allan standard deviation over times scales from 1 to 1000 seconds. The results for the 16-channel averaged data are shown in **Figure 8**. The data were fitted to a power law with strong correlation, with a best-fit power law of -0.69.

978-1-4673-1813-6/13/$31.00 ©2013 IEEE

Following Treuhaft & Lanyi [9], we interpret this as Kolmogorov turbulence static spatial fluctuations carried over the site by a ~10 m/s wind (frozen flow). Under these assumptions, for points separated by more than the wet troposphere scale height of ~2km, one expects 2-D turbulence to produce a tropospheric fluctuation power law of -2/3 [9].

On time scales more than ~1200 sec the Allan deviation is dominated by 2-D tropospheric turbulence—even at night on this short ~10km baseline. The plateau between 25 and 75 seconds may be an indication of 3-D tropospheric variation generated by fluctuations close than the 2km scale height (theoretical slope -1/6). For time scales from 1 to 25 seconds the steeper than average slope may indicate that we are starting to be limited by white noise (theoretical slope -1). Given that we did not see the Allan deviation flatten out or turn up, we conclude that the phase errors in this experiment were dominated by the troposphere fluctuations rather than by instrumental errors. In summary, the PRSR's stability was so good that it was below our ability to measure it with this experimental configuration.

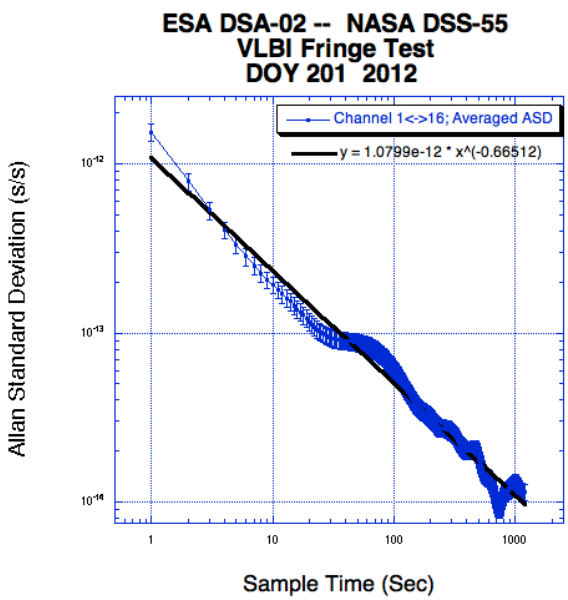

Figure 8- Allan standard deviation, DSS-55 and DSA-02

7. Analysis of Malargüe Data

Data

The successful demonstration with the Madrid-Cebreros baseline gave us the confidence to proceed to Malargüe, Argentina. The PRSR was shipped and arrived just before DSA03 became operational. This time we paired Malargüe, Argentina with Tidbinbilla, Australia (DSS-34). We recorded our first scientifically interesting data using the Tidbinbilla- Malargüe baseline on DOY 347. As with Madrid-Cebreros, we recorded Ka-band (32 GHz) with 16 channels of 4-MHz wide data at 2-bit resolution spanning 180 MHz. We tracked P 1034-293 for 2030 seconds and calculated Allan deviation to measure system stability.

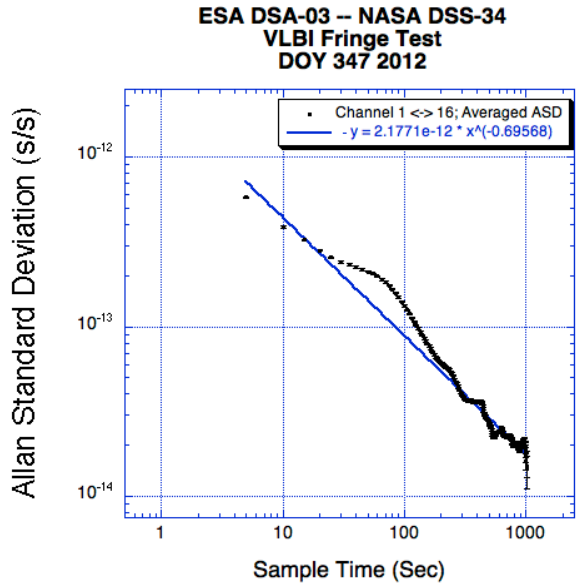

Figure 9- Allan standard deviation, DSS-55 and DSA-03

The Allan standard deviation for the 16-channel averaged data is shown in **Figure 9**. The data were fitted to a power law with strong correlation, yielding a slope of -.64, very close to the Kolmogorov frozen flow model value of -.67. The data has an unexplained bump from ~ 30 sec to 300 sec. The slope at low sample times (< 30 sec) yields a power law of ~-1/2. The high sampling side of the bump ([90,550sec] has a power law fit very close to -1, white noise. The overall appearance of the Allan standard deviation on both the short Madrid-Cebreros baseline and long Tidbinbilla-**Malargüe** is about the same. However, the remaining error term is a factor of two greater on the Tidbinbilla-**Malargüe** baseline. This difference is presumably due to the true independence of the troposphere on the very long baseline.

Future Applications

Using Delta-DOR, two-dimensional angular position requires measurements from two baselines with orthogonal components. As shown in **Figure 2**, a mission in the southern sky could be fully supported by the DSN Goldstone-Canberra baseline combined with either the ESA New Norcia-Cebreros baseline or the mixed Goldstone-Malargüe baseline. Further, an all-southern baseline such as mixed Canberra- Malargüe would be useful for a mission in the southern sky.

Navigating a lander safely to its destination on another planet is arguably the most demanding navigation task that we undertake. Given that NASA's Deep Space Network is biased toward northern stations, any lander mission in the southern hemisphere is even more difficult. The 2012 MSL

978-1-4673-1813-6/13/$31.00 ©2013 IEEE

lander encountered Mars at -10 degrees declination as seen from Earth and is just such a case. NASA's 2016 InSight mission is an even more difficult geometry with its encounter with Mars occurring at -26 deg declination as seen from Earth. This is so far south that for VLBI, the California to Spain baseline is too far north to be of any practical use. Therefore, we anticipate that cooperative ESA-NASA VLBI baselines from Goldstone, Madrid, and especially Canberra each to Malargüe, Argentina will be of great value in improving our tracking geometry.

8. CONCLUSION

We have designed, built, and tested a Portable Radio Science Receiver which bridges the NASA and ESA networks allowing them to be combined into a united super-network. The modest cost, configuration flexibility, and portability of the PRSR allows it to contribute to VLBI tracking measurements and reference frame infrastructure, as well as MSL EDL and GRAIL applications. We field demonstrated the PRSR by tying together the ESA site in Cebreros, Spain with the NASA site in Robledo, Spain. The proximity of these operational sites maximized our ability for cross-agency interaction and problem solving. The result was a 2cm (1-sigma, per 3-D component) tie for the ESA and DSN station location systems. Using an Allan variance test, we demonstrated that the PRSR instrumentation was so stable that it was below atmospheric instabilities even on a very short 10km baseline. As a result, the PRSR phase stability is not expected to be a limiting factor in future measurements.

We also made the first Ka-band VLBI measurements on a Tidbinbilla, Australia to Malargüe, Argentina baseline. The PRSR's use with the Malargüe, Argentina ESA station will form three new baselines, improving the radio catalog in the southern hemisphere and enabling Delta-DOR measurements with an accuracy of better than 200 μas in the mid to far south. This is now the highest resolution astronomical instrument ever operated solely from the Southern Hemisphere. These measurements will improve spacecraft tracking and navigation, particularly for low declination missions such as InSight.

9. ACKNOWLEDGEMENTS

The authors would like to acknowledge the contribution of Robert Proctor in the implementation and delivery of the PRSR. The authors would also like to thank Jim Border for his valuable review and motivation for improvements to Delta-DOR, Jesus Alonzo, Luis Gamborino, and Ioana Sotuela for excellent support and operations of the PRSR at DSA-02, Michel Dugast, Shinji Horiuch, and Phil Pope for their contributions in recording the DOY 347 data, Ladislao Saldana for handling experiment logistics, and Steve Lowe for providing signal processing software. Lastly, thanks to Faramaz Davarian for facilitating the travel of the PRSR to DSA-02 and DSA-03 and making this work possible.

This research was carried out at the Jet Propulsion Laboratory, California Institute of Technology. Copyright 2012 all rights reserved. Government sponsorship acknowledged.

978-1-4673-1813-6/13/$31.00 ©2013 IEEE

REFERENCES

[1] Asmar, S. W., Armstrong, J. W., Iess, L., and Tortora, P., "Spacecraft Doppler tracking: Noise budget and accuracy achievable in precision radio science observations," *Radio Science* 40, RS2001, 2005.

[2] C. L. Thornton and J.S. Border, Radiometric Tracking Techniques for Deep Space Navigation, Monograph 1, Deep Space Communications and Navigation Series, Jet Propulsion Laboratory, California Institute of Technology, Pasadena, California, 85 p, 2000.

[3] G. Lanyi, D. S. Bagri and J. S. Border, "Angular Position Determination of Spacecraft by Radio Interferometry," Proceedings of the IEEE, vol. 95, no. 11, p. 2193, November 2007.

[4] C.S. Jacobs, J.E. Clark, C. García-Miró, S. Horiuchi, A. Romero-Wolf, L.G. Snedeker, I. Sotuela, "A Celestial Reference Frame at X/Ka-band (8.4/32 GHz) for Deep Space Navigation," 23rd International Symposium on Space Flight Dynamics, Pasadena CA, 30 Oct 2012. https://issfd.jpl.nasa.gov/home/assets/papers/ISSFD23_IMD1_1.pdf

[5] A. Kwok. "Open-Loop Radio Science." DSN Telecommunications Link Design handbook, 810-005. June 1, 2010.

[6] M. Soriano, S. Finley, A. Jongeling, D. Fort, C. Goodhart, D. Rogstad, R. Navarro, "Spacecraft-to-Earth Communications for Juno and Mars Science Laboratory Critical Events," Proc. IEEE Aerospace Conference, MT, March 2012.

[7] S. Rogstad, R. Navarro, S. Finley, C. Goodhart, R. Proctor, and S. Asmar, "The Portable Radio Science Receiver (RSR)," The Interplanetary Network Progress Report, vol. 42-178, Jet Propulsion Laboratory, Pasadena, California, pp. 1–7, August 15, 2009.

[8] E. Vassallo, R. Martin, R. Madde, M. Lanucara, P. Besso, P. Droll, G. Galtie, J. De Vicente, "The European Space Angency's Deep-Space Antennas," Proceedings of the IEEE, vol. 95, no. 11, p/ 2111, November 2007.

[9] R.N. Treuhaft and G. E. Lanyi, "The effect of the dynamic wet troposphere on radio interferometric measurements," *Radio Science* vol. 22, p, 251, 1987.

[10] R. Navarro, J. Bunton, "Signal Processing in the Deep Space Array Network," The Interplanetary Network Progress Report, vol. 42-157, Jet Propulsion Laboratory, Pasadena, California, pp. 1–17, May 15, 2004

[11] S. Lowe, "SOFTC: A Software VLBI Correlator," JPL Section 335 internal document, Jet Propulsion Laboratory, Pasadena, CA, 29 April 2005. http://adsabs.harvard.edu/abs/2006ntb..rept...43L

[12] S. Lowe, "Theory of Post-BlockII VLBI Observable Extraction," JPL Publication 92-7, Jet Propulsion Laboratory, Pasadena CA, 15 July 1992. http://ntrs.nasa.gov/archive/nasa/casi.ntrs.nasa.gov/19940009399_1994009399.pdf

978-1-4673-1813-6/13/$31.00 ©2013 IEEE

Melissa Soriano *is a staff software engineer in the Tracking Systems and Applications Section at the Jet Propulsion Laboratory. She has developed real-time software for Direct-To-Earth communications with Mars Science Laboratory during Entry, Descent, and Landing, the Long Wavelength Array, NASA's Breadboard Array, and the Wideband VLBI Science Receiver used in the Deep Space Network. Melissa is also currently the software cognizant engineer for the DSCC Downlink Array. She has a B.S. from Caltech, double major in Electrical and Computer Engineering and Business Economics and Management. She also has an M.S. in Computer Science from George Mason University.*

Christopher S. Jacobs *received the B.S. degree in applied physics from California Institute of Technology, Pasadena, in 1983. He is a Senior Engineer with the Deep Space Tracking Systems Group, Jet Propulsion Laboratory, Pasadena. His work has centered on producing quasi-inertial reference frames based on observations f extragalactic radio sources. These frames define the angular coordinates used for spacecraft navigation. He has served on IAU working groups for celestial reference frames as a co-author of the paper that introduced the extragalactic radio frame (ICRF) as a replacement for optically based definitions of celestial angular coordinates. His recent research interests have focused on extending the ICRF to higher radio frequency bands such as 24, 32, and 43 GHz. Mr. Jacobs is a member of AAS and the IAU.*

Robert Navarro *is the deputy manager of the Telemetry, Tracking and Command, End-to-End Data Services Office for the Deep Space Network at JPL. He received a B.S in Engineering from Harvey Mudd College in 1986 and a M.S. in Electrical Engineering in 1987. Since 1991, his work at JPL has centered on signal processing for DSN ground systems such as full spectrum antenna arrays, VLBI correlators and data acquisition systems and radio science open loop data recorders. He led a team in developing a Digital Processing Subsystem for the University of New Mexico's Long Wavelength Array and worked on a radio transient detection system for large arrays of radio telescopes in collaboration with the International Centre for Radio Astronomy Research.*

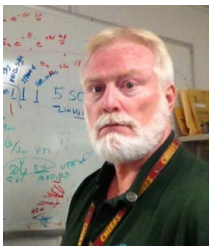

Charles Naudet *received the B.S. degree in Engineering Physics from the University of Kansas in 1979, the M.S. degree in Physics from Rice University, Houston Texas, in 1983, and the Ph.D. degree from Rice University in 1986. From 1986 to 1993, he worked in the Nuclear Science Division at Lawrence Berkeley Laboratory (LBL). While at LBL, he served first as a post-doctoral research assistant then as a member of the research staff studying di-electron production in nucleus-nucleus interactions. In 1993 he joined the Jet Propulsion Laboratory as a member of the technical staff supporting astrometric measurements of quasars and spacecraft. In 1999 he was promoted to a member of the senior staff and from 2003 until the present is the group supervisor of the Deep Space Tracking Systems group at JPL. He is the manager of the Interplantary Network Directorate Radiometrics Technology work area, a co-investigator of ANITA (Antarctic Impulsive Transient Antenna) and currently is involved in the study of Giant Pulses from the Crab pulsar.*

Stephen Rogstad *is the group supervisor of the Processor Systems Development Group (PSDG) at JPL. He received his B.S. and M.S. degrees in Electrical and Computer Engineering from the California State Polytechnic University in Pomona with an emphasis in digital signal processing and filter design. Steve joined JPL in 1994 and the PSDG group in 2001, where he has worked as a signal analysis engineer for open loop receivers and antenna arraying systems. Steve has recently been the task manager for several projects including the Wideband VLBI Science Receiver (WVSR), the Deep Space Communications Complex (DSCC) VLBI processor (DVP), and the DSCC downlink Array (DDA).*

Leslie White *is cognizant engineer for the PRSR and was instrumental in its successful operation at DSA-03 in Malargüe, Argentina. He received his BSEE from UCLA and specializes in spacecraft and DSN ground systems design, including antenna arrays and open-loop receivers. Les has been at JPL for 30+ years.*

978-1-4673-1813-6/13/$31.00 ©2013 IEEE

Susan Finley *is a key staff member in the Processor Systems Development Group at JPL. She is the subsystem engineer for the Full Spectrum Processor subsystem deployed in NASA's Deep Space Network. Her experience includes the operation of the EDA for both of the MER landings on Mars as well as the operation of the Radio Science Receiver for the landing of the Huygens Probe on Titan and for the Phoenix landing on Mars.*

Charles Goodhart *is a senior staff software engineer in the Processor Systems Development Group at JPL. He received a B.S. and M.S. in Applied Mathematics from Caltech. He joined JPL in 1985 to work on the Hypercube Parallel Processor Supercomputer Project and served as the Cognizant Engineer for the Crystaline Operating System (CrOS). He has contributed to a number of high performance computing projects and, most recently has worked on DSN ground systems for radio science and VLBI recording.*

Elliott Sigman *has a Ph.D. in Electrical Engineering from University of Michigan. A former professor at Harvey Mudd College, he has been at the Jet Propulsion Laboratory for 30 years. He is accomplished in many areas of electronic design including RF, analog, high speed digital, A/D conversion, high speed ECL circuitry, FPGA design, high speed printed circuit board design, and digital signal processing design. He has done top level system design along with the detailed circuit design, printed circuit board design, firmware design, and software code generation for phase calibration systems, and deep space probe receivers which have been in use in JPL's Deep Space Network for over 15 years.*

Joseph T. Trinh *joined NASA's Jet Propulsion Laboratory at the California Institute of Technology in 2000. He received his Bachelor of Science in Computer and Electrical Engineering from the California State Polytechnic University, Pomona in 2002. As a computer and electrical engineer, he has been working with the Processor System Development Group in hardware and firmware designs.*

Roberto Maddè *received the laurea degree in electronic engineering from Politecnico di Milano, Milan, Italy, in 1985. He joined FIAR Spa, Space Division (now Galileo Avionica), Milan, in 1986, where he was involved in several space projects. He joined the European Space Operations Centre, European Space Agency (ESA), Darmstadt, Germany, in 1989, where he has been responsible for the development of all equipment installed in ESA tracking telemetry and command systems ground stations. He is currently the Project Manager of the ESA's Third Deep Space Station, recently inaugurated in Argentina.*

978-1-4673-1813-6/13/$31.00 ©2013 IEEE